**Electronic Supporting Information**

# Rationale for the crystallization of titania polymorphs in solution

N. Kränzlin,[a] M. Staniuk,[a] F. J. Heiligtag,[a] L. Luo,[a] H. Emerich,[b] W. van Beek,[b] M. Niederberger,[a] and D. Koziej[a]*

[a] Laboratory for Multifunctional Materials, Department of Materials, ETH Zürich, Vladimir-Prelog-Weg 5, 8093 Zürich, Switzerland
[b] Swiss-Norwegian Beamlines at European Synchrotron Research Facility, 6 Rue Jules Horowitz, 38043 Grenoble, France
* Corresponding author: dorota.koziej@mat.ethz.ch

***Data recording.***

(a) PXRD patterns of powders obtained in the control experiment under laboratory conditions were recorded on the X'Pert Pro (PANalytical B. V., Netherlands) powder diffractometer operating in reflection mode with Cu $K_\alpha$ radiation (45 kV, 40 mA).

(b) A schematic representation of the setup used for the in-situ studies is given in Figure S1. The PXRD and XAS data were collected almost simultaneously at the Swiss Norwegian Beamline (SNBL) at the European Synchrotron Radiation Facility (ESRF) in Grenoble. The delay time between the PXRD and XAS scans is the time needed to record a given scan. PXRD data were collected using a wavelength of 0.503433 Å. The beam spot size at the front window of the sample cell containing the reaction solution was ~0.7 mm × ~0.7 mm and the beam passed through the sample over a length of ~5 mm. The sample volume was constantly irradiated during the time of reaction. The arm of High Resolution Powder Diffractometer holds a vertical array of six independent Si-111 analyzers. Each analyzer is followed by its own scintillation counter for single photon counting. The diffracted X-rays from the sample are diffracted a second time on the analyzer crystal before being detected. Data from a monitor counter, placed in front of the sample, was used to normalize the measured intensities for beam decay. Such a setup ensures at all times that reliable lattice parameters are measured. The angular spacing between these six channels is 1.1 degrees. To monitor fast changes in the beginning, high time- and spatial-resolution is needed, therefore the 2 theta range was limited to capture the (101) and (110) reflections of anatase and rutile respectively (7 ° to 11 °). Upon stabilization of the system towards the end of reaction six long-range PXRD scans were performed (7 ° to 40 °). XAS measurements were recorded with a Vortex EM fluorescence detector readout by Xia digital electronics. The step size of the Ti K-edge X-ray absorption near edge structure (XANES) scans was 0.2 eV and was maintained also during the recording of the extended X-ray absorption fine structure (EXAFS) patterns.

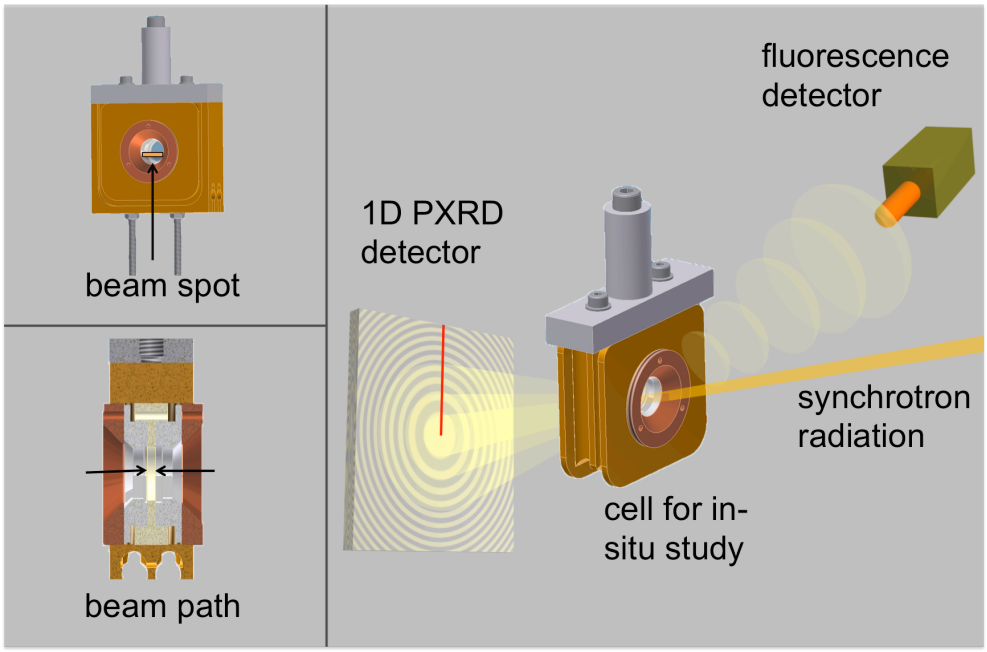


**Figure S1.** Schematic of the measurement cell. The synchrotron beam irradiated a cuboid shaped volume of the reaction solution, which was entrapped between two Kapton windows and remained constant. The diffracted X-rays were collected behind the measurement cell on a 6 crystal analyzer array to monitor ongoing crystallization, whereas fluorescence radiation was detected in front of the cell for elucidating changes in atomic distances and oxidation states in structures lacking in long-range periodic order.

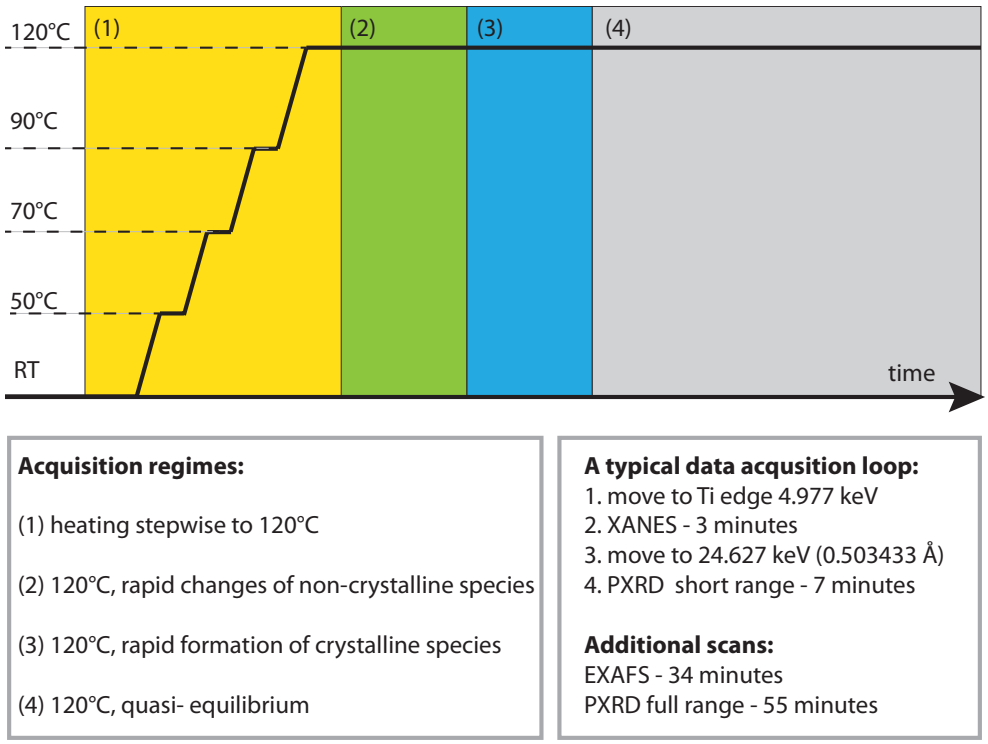


**Figure S2.** The different stages of the in-situ experiment. (1) The reaction solution is heated step by step to the final reaction temperature of 120 °C. Meanwhile PXRD scans are performed under isothermal conditions at the indicated temperatures. In regions (2) and (3) where rapid changes of non-crystalline species and rapid formation of crystalline species respectively demand fast data acquisition, recording loops as described to the lower right are run. (4) As soon as the system reaches quasi equilibrium condition, additional long time scans are conducted.

***Data handling***. For evaluating the diffractograms recorded from 7 ° to 11 °, single peak and where needed double peak fitting routine was applied in order to extract full width at half maximum (FWHM) and peak intensity values. The peak analyzer function within the OriginPro[1] software package was used to fit a pseudo-voigt profile to the single or double peaks. Indexing of the initially formed $Ti(OH)_xCl_{4-x}$ crystal phase was done using the program TREOR[2] implemented in the software CMPR[3] (the elemental analysis of the precipitate without any washing or purification confirmed the presence of Ti, O, H, Cl and additionally C, being residuals of acetone). Full pattern fits of the long range PXRD scans were done in FullProf[4] by refining only for lattice parameters, overall Debye-Waller factors and crystallite sizes. To correct for anisotropy we introduced the spherical harmonics approach as it was also successfully implemented by others.[5-6] For picturing the directional crystal sizes the extension perpendicular to the corresponding lattice planes from which the FWHM values were extracted was calculated using the Scherrer equation attributing the peak widening solely to crystallite size effect. The corresponding points were connected in the a, b, c coordinate system using convex hull algorithm provided in the software package TetGen[7] together with ParaView[8] for visualization. For EXAFS data treatment the software packages WINXAS Version 3.2[9] and Athena Version 0.8.056[10-11] are used. No energy correction was performed on the spectra since only the spectra recorded in-situ were compared. After deglitching, the data were normalized with pre-edge range from -31.895 eV to -17.486 eV and normalization range from 150 eV to 931 eV. $E_0$ is set to 4977.22 eV for all measurements (see Figure S6). To receive the radial distribution a Fourier transformation with Bessel window from 1 $Å^{-1}$ – 12 $Å^{-1}$, a window parameter of 10 and k-weight of 1 is used. XANES spectra in the energy range of 4949.8 – 5006.8 eV, recorded during first 700 minutes of reaction were analyzed with the MCR-ALS method. The data processing was done analogously to procedure described elsewhere.[12] The number of components was chosen on the basis of Singular Value Decomposition (SVD) results and the initial estimates of spectra of components were based on SIMPLISMA method with the noise level set to 5 %. The ALS algorithm with following constraints was applied: (1) non-negativity of spectra and concentrations, (2) unimodality of concentrations (tolerance: 20 %), (3) convergence criterion: 0.1. The SVD results show that increasing the number of components from 3 to 4 will result only in a minor increase of the explained variance in the data (see Figure S7 and Table S1). Therefore we choose 3 components to explain our data. Table S2 presents the lack of fit values, the variance explained and the standard deviation of residuals respect experimental data obtained after ALS optimization.[13]

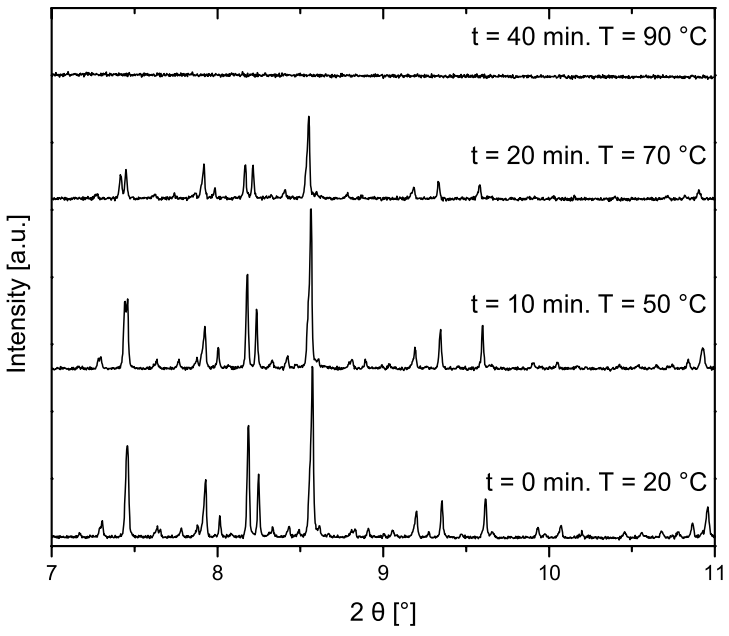


**Figure S3.** PXRD patterns revealing the initial dissolution of the monoclinic $Ti(OH)_xCl_{4-x}$ crystal phase upon heating the reaction solution up to 120 °C. The diffraction pattern recorded at 20 °C could be indexed on a primitive monoclinic unit cell (a = 13.237 Å, b = 14.853 Å, c = 7.621 Å, β = 97.069°). A careful examination of the diffraction pattern indicated that (1) h0l reflections with h + l = 2n + 1; and (2) 0k0 reflections with k = 2n + 1 were systematically absent, so the space group P21/n was expected.

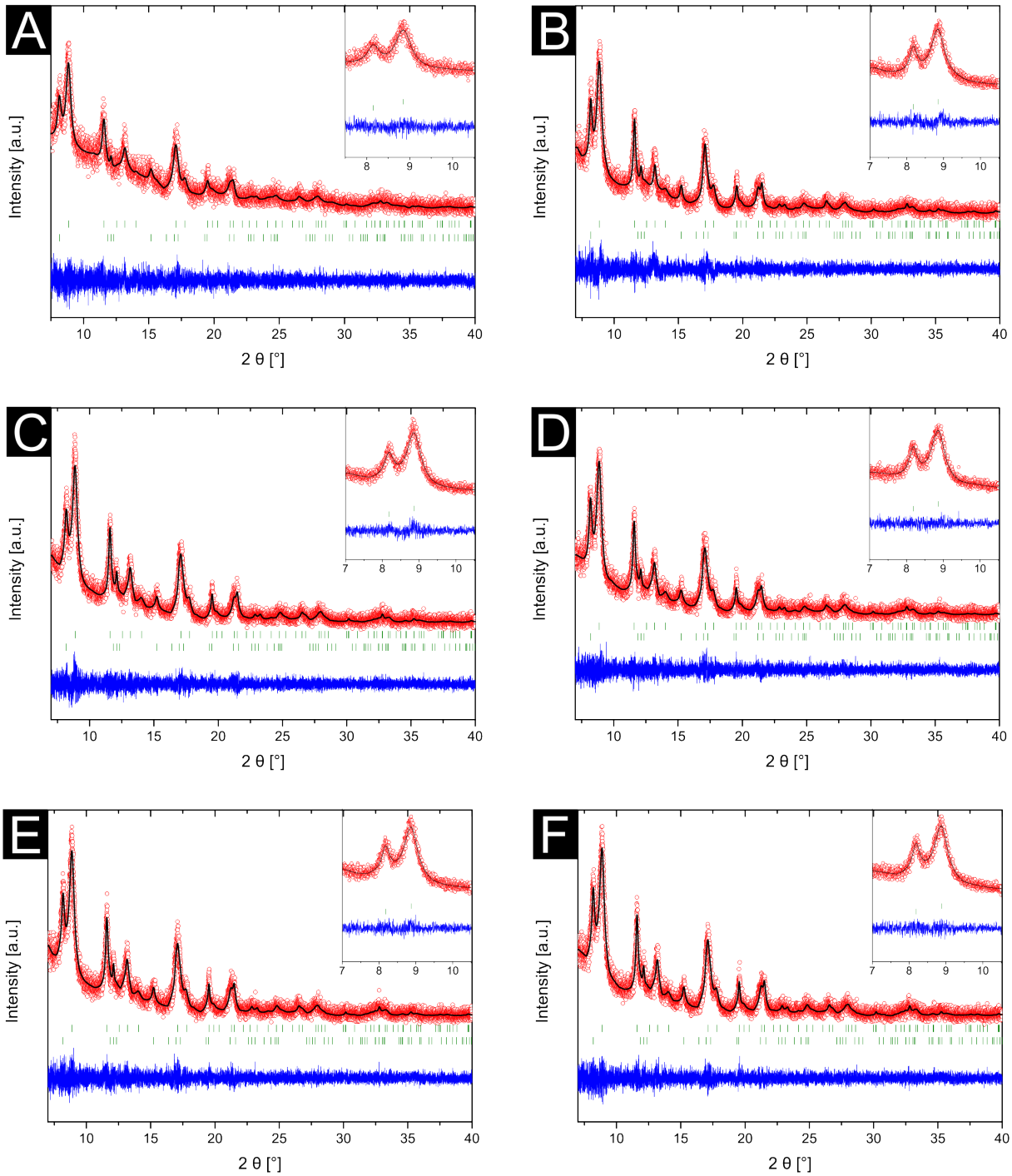


**Figure S4.** Full pattern fits of the long range PXRD scans, which were done in FullProf by refining only for lattice parameters, overall Debye-Waller factors and crystallite sizes after (A) 1420 minutes, (B) 2440 minutes, (C) 2680 minutes, (D) 3160 minutes, (E) 3520 minutes and (E) 4000 minutes.

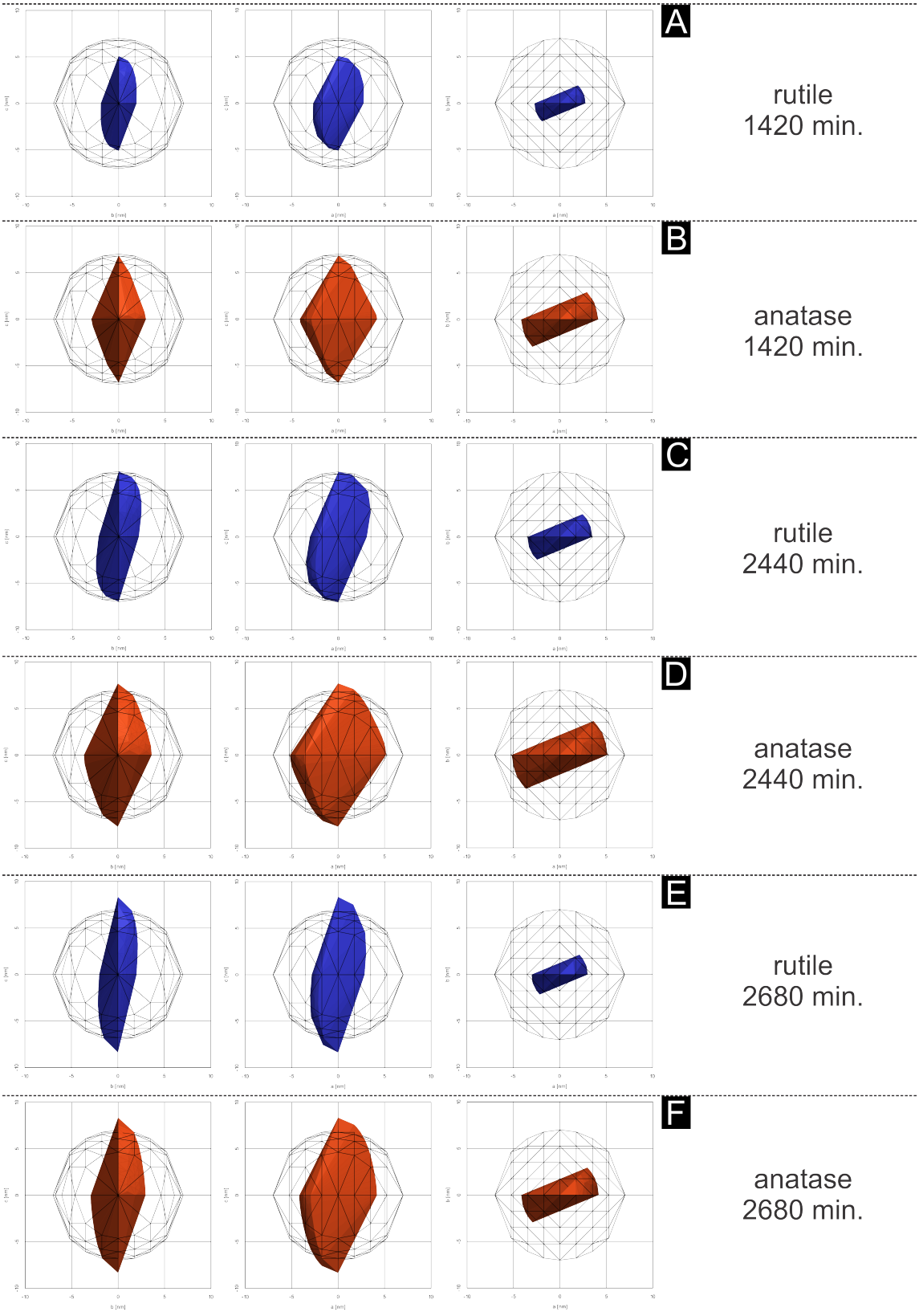


**Figure S5.** A.-F. The contoured orthogonal projection on (left) a,b, (middle) a,c and (right) b,c planes of size of anatase (orange) and rutile( blue) based on the widening of all indexed reflections at different reaction times between 1420 and 2680 min.

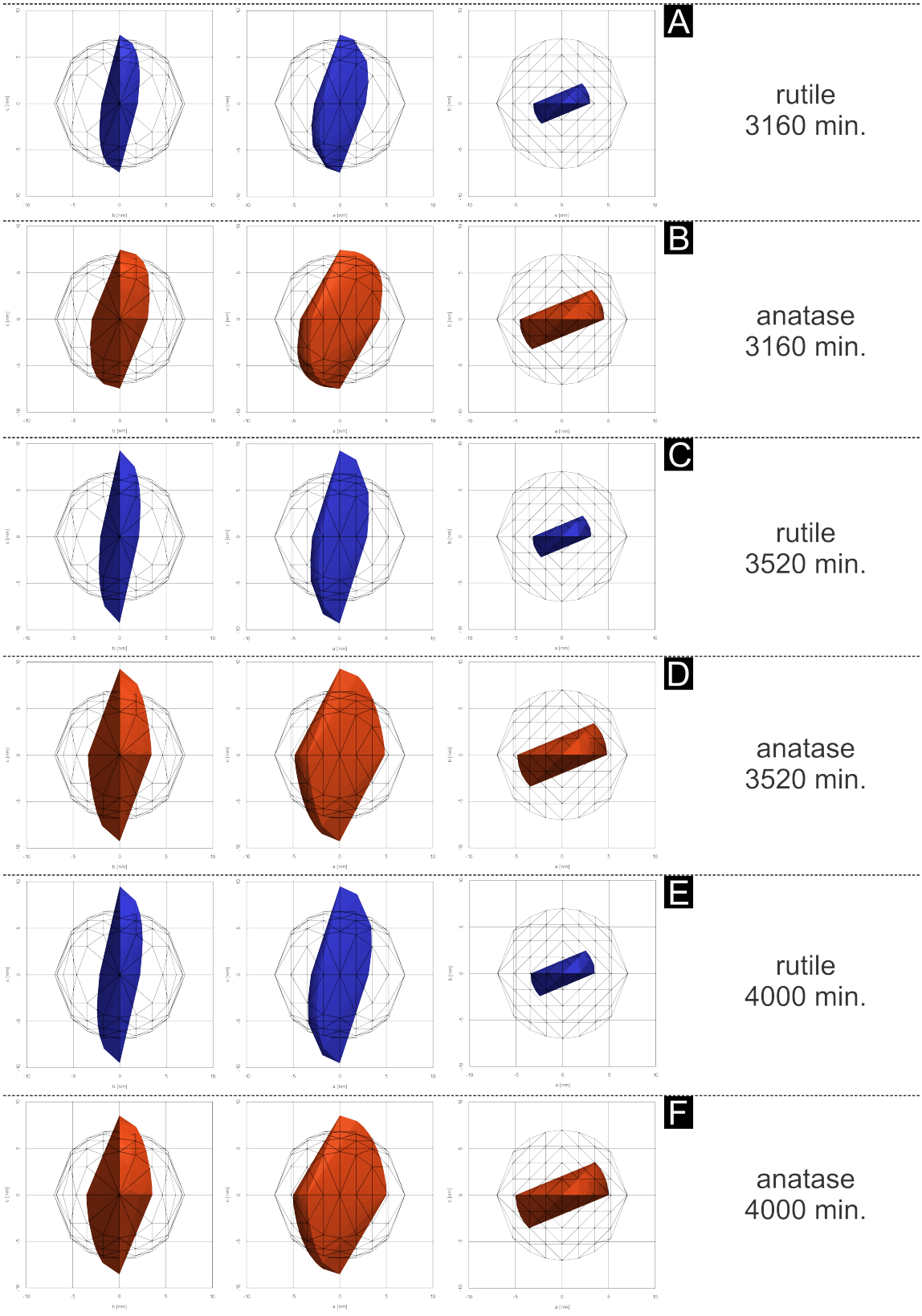


**Figure S6.** A.-F The contoured orthogonal projection on (left) a,b, (middle) a,c and (right) b,c planes of size of anatase (orange) and rutile( blue) based on the widening of all indexed reflections at different reaction times between 3160 and 4000 min.

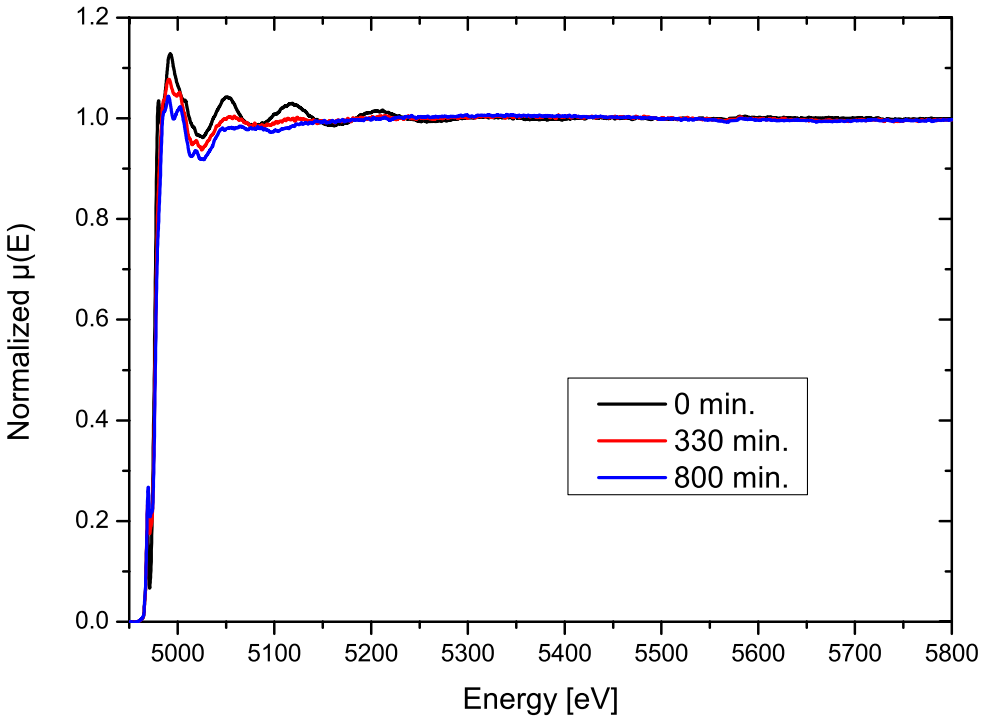


**Figure S7.** Normalized EXAFS spectra recorded in-situ at corresponding times of reaction.

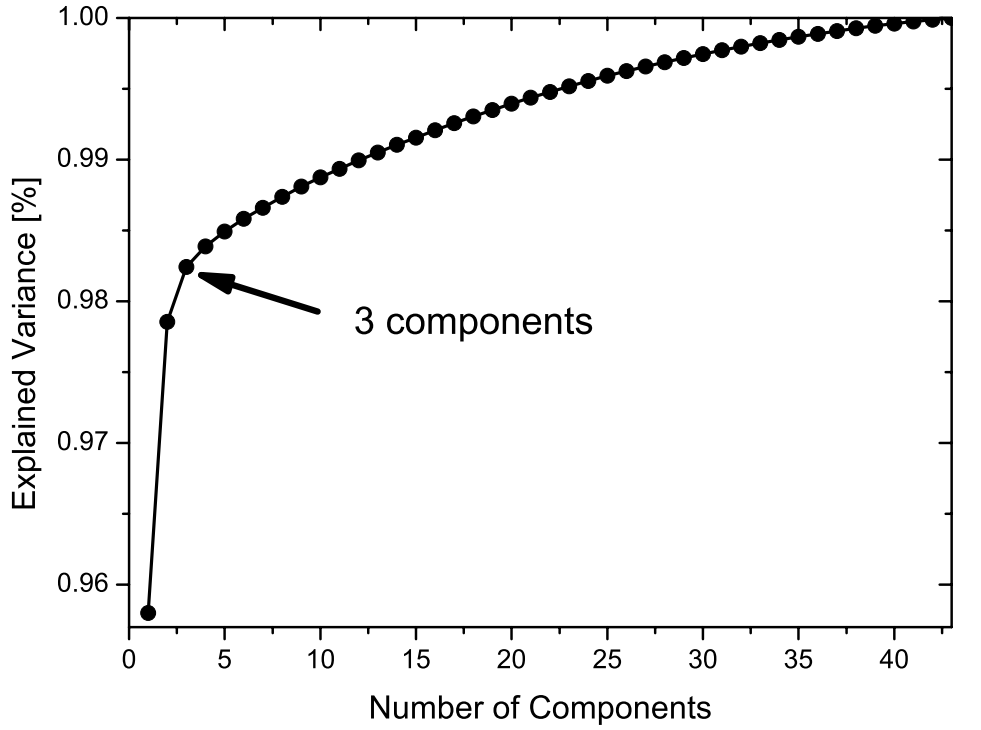


**Figure S8.** MCR-ALS of XAS. Variance explained according to different numbers of components from Table S2.

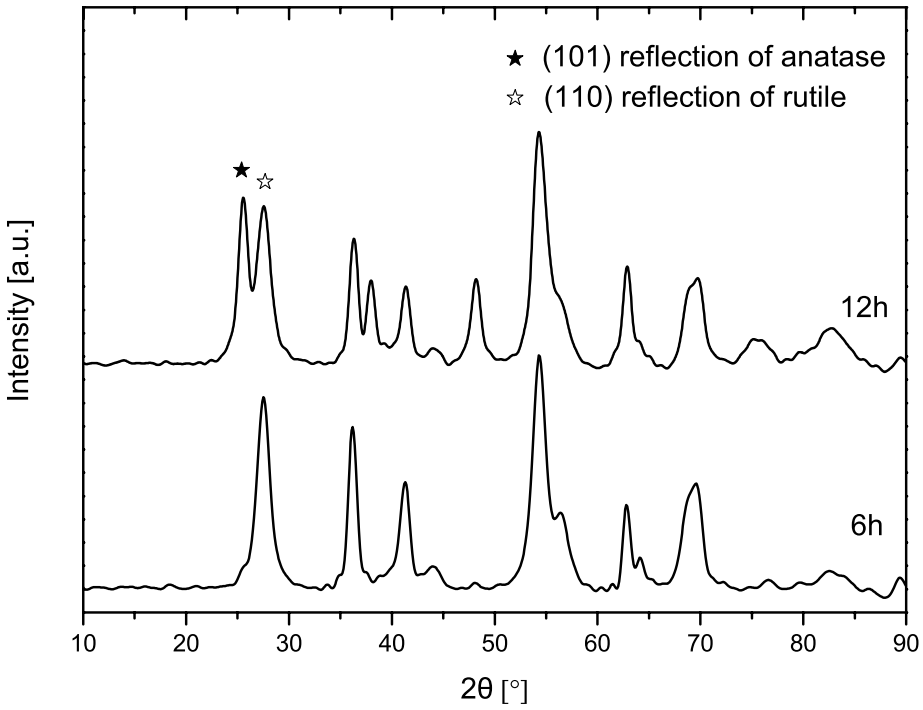


**Figure S9.** Ex-situ control experiment showing the presence of rutile $TiO_2$ after 6 hours and co-existence of rutile and anatase $TiO_2$ after 12 hours of reaction.

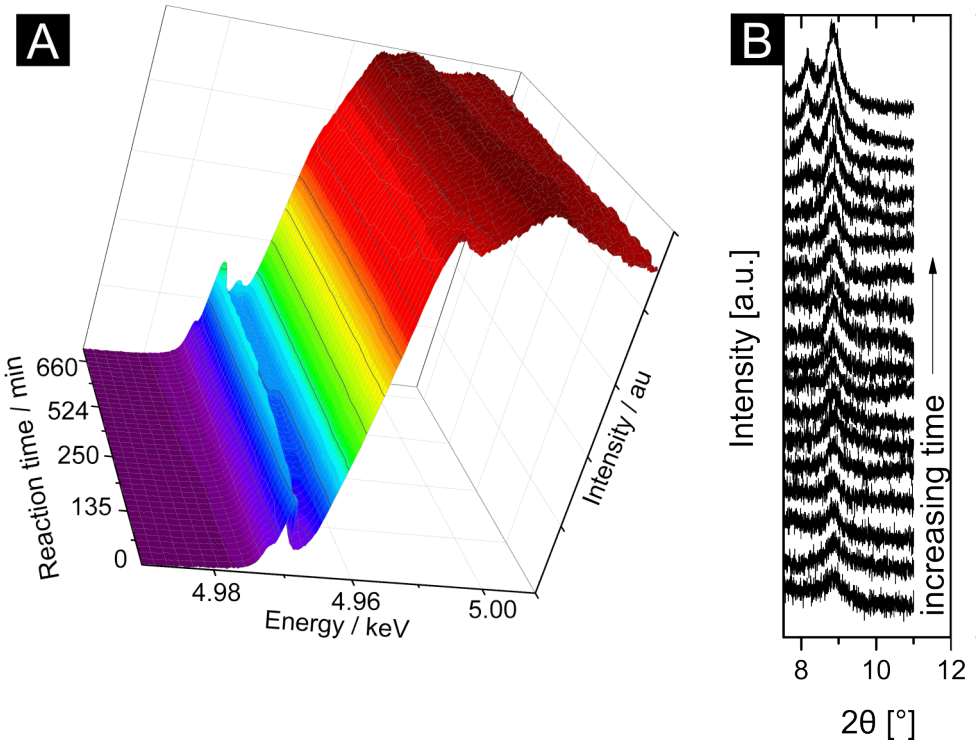


**Figure S10.** (A) XAS and (B) PXRD raw data recorded during the first 1420 minutes of reaction. Referring to Figure 1 the XAS data were recorded in phase (2) and the PXRD data in phase (3).

**Table S1.** The first ten eigenvalues of data matrix calculated by Singular Value Decomposition and the variance in the data that can be explained by choosing certain number of components. The threshold was set after third value highlighted in red.

| Number of components | Eigenvalues | Variance explained |
|---|---|---|
| 1 | 48.5033 | 0.957999 |
| 2 | 1.0405 | 0.978550 |
| 3 | 0.1956 | 0.982414 |
| 4 | 0.0744 | 0.983883 |
| 5 | 0.0533 | 0.984936 |
| 6 | 0.0451 | 0.985827 |
| 7 | 0.0394 | 0.986605 |
| 8 | 0.0387 | 0.987369 |
| 9 | 0.0376 | 0.988112 |
| 10 | 0.0324 | 0.988752 |

**Table S2.** The lack of fit values, the variance explained and the standard deviation of residuals with respect to the experimental data obtained after ALS calculation of in-situ XANES data.

| | |
|---|---|
| $lof_{ALS}$ | 1.7225 % |
| $lof_{PCA}$ | 1.7561 % |
| $R^2$ | 99.9692 |
| σ | 0.015001 |

**References:**


1 *OriginPro v. 8.6.0, OriginLab Corporation USA*

2 P. E. Werner, L. Eriksson and M. Westdahl, *J. Appl. Crystallogr.,* 1985, **18**, 367.

3 B. H. Toby, *J. Appl. Crystallogr.,* 2005, **38**, 1040.

4 J. Rodríguez-Carvajal, *FullProf version 5.03 March 2012 - ILL JRC.*

5 M. Jarvinen, *J. Appl. Crystallogr.,* 1993, **26**, 525.

6 E. D. Bøjesen, K. M. Ø. Jensen, C. Tyrsted, N. Lock, M. Christensen and B. B. Iversen, *Cryst. Growth Des.,* 2014, **14**, 2803.

7 S. Hang, *TetGen v. 1.5 downloaded from* http://www.tetgen.org.

8 *ParaView v. 4.1.0 downloaded from* http://www.paraview.org.

9 T. Ressler, *J. Synchrotron Radiat.,* 1998, **5**, 118.

10 B. Ravel and M. Newville, *J. Synchrotron Radiat.,* 2005, **12**, 537.

11 M. Newville, *J. Synchrotron Radiat.,* 2001, **8**, 322.

12 M. Staniuk, O. Hirsch, N. Kränzlin, R. Böhlen, W. van Beek, P. M. Abdala and D. Koziej, *Chem. Mater.,* 2014, **26**, 2086.

13 J. Jaumot, R. Gargallo, A. de Juan and R. Tauler, *Chemom. Intell. Lab. Syst.,* 2005, **76**, 101.